

## FAST AND EXACT SIMULATION OF STATIONARY GAUSSIAN PROCESSES THROUGH CIRCULANT EMBEDDING OF THE COVARIANCE MATRIX\*

C. R. DIETRICH<sup>†</sup> AND G. N. NEWSAM<sup>‡</sup>

**Abstract.** Geostatistical simulations often require the generation of numerous realizations of a stationary Gaussian process over a regularly meshed sample grid  $\Omega$ . This paper shows that for many important correlation functions in geostatistics, realizations of the associated process over  $m + 1$  equispaced points on a line can be produced at the cost of an initial FFT of length  $2m$  with each new realization requiring an additional FFT of the same length. In particular, the paper first notes that if an  $(m+1) \times (m+1)$  Toeplitz correlation matrix  $R$  can be embedded in a nonnegative definite  $2M \times 2M$  circulant matrix  $S$ , exact realizations of the normal multivariate  $y \sim \mathcal{N}(0, R)$  can be generated via FFTs of length  $2M$ . Theoretical results are then presented to demonstrate that for many commonly used correlation structures the minimal embedding in which  $M = m$  is nonnegative definite. Extensions to simulations of stationary fields in higher dimensions are also provided and illustrated.

**Key words.** geostatistics, Monte Carlo simulations, time series, random fields

**AMS subject classifications.** 86A32, 65C05, 65C10, 62M40, 65U05

**PII.** S1064827592240555

**1. Introduction.** Monte Carlo simulations in geostatistics often require the generation of a large number of realizations of a stationary Gaussian process on a discrete mesh of sample points  $\Omega$ . For example, random processes are often invoked in hydrogeology to model highly variable quantities, such as the hydraulic conductivity of a groundwater formation (RamaRao et al. [23]; King and Smith [17]). Monte Carlo simulations are also used to quantify uncertainty in the output of nonlinear models that depends on parameters viewed as normal random variables (Sposito, Jury, and Gupta [26]).

Such realizations can be obtained in various ways. In one dimension perhaps the two most commonly used approaches are matrix factorization techniques (Davis [7]) and spectral methods (Shinozuka and Jan [25]; Borgman, Taheri, and Hagan [4]). In higher dimensions, the turning bands method is often preferred because of its computational efficiency (Mantoglou and Wilson [19]; Tompson, Ababou, and Gelhar [27]). Nevertheless, as the turning bands method generates multidimensional realizations from appropriately summed line realizations, it still requires an auxiliary algorithm for generating these line realizations; this is often a spectral method.

All of the above methods have their particular drawbacks; in essence the choice between them usually boils down to a trade-off between speed and accuracy. The purpose of this paper is to present a new algorithm for generating stochastic simulations that is both fast and accurate. To motivate our algorithm, we first briefly review the matrix factorization and spectral methods as our approach can be viewed as a synthesis of these two approaches. We shall take as the canonical problem that of generating realizations of a stationary Gaussian process  $Y(x)$  with zero mean and

\*Received by the editors November 18, 1992; accepted for publication (in revised form) October 20, 1995.

<http://www.siam.org/journals/sisc/18-4/24055.html>

<sup>†</sup>Division of Australian Environmental Sciences, Griffith University, Nathan, Queensland 4111, Australia (c.dietrich@ens.gu.edu.au).

<sup>‡</sup>Information Technology Division, Defence Science and Technology Organisation, P.O. Box 1500, Salisbury, S.A. 5108 Australia (g.newsam@itd.dsto.gov.au).

prescribed covariance on a set of equispaced points  $\Omega = \{x_0, \dots, x_m\}$  on the line. We further assume that the variance of the process at all points is unity, so that the covariance and correlation structures of the process are identical. By definition, in a stationary process the correlation is invariant under translation. Therefore the correlation  $E[Y(x)Y(y)]$  between any two points  $x$  and  $y$  can be characterized by a correlation function  $r(|x|)$  in that the expectation  $E[Y(x)Y(y)] = r(|x - y|)$ . Thus we wish to generate instances of the vector  $y = (Y(x_0), \dots, Y(x_m))^T \sim \mathcal{N}(0, R)$  with the correlation matrix  $R$  having entries  $R_{pq} = r(|x_p - x_q|)$ .

The matrix factorization approach to generating realizations of  $y$  is based on factoring the correlation matrix  $R$  into the product  $R = AA^T$ . Then if  $\epsilon \sim \mathcal{N}(0, I)$  is a vector of  $m + 1$  zero mean, uncorrelated random variables, the vector  $y = A\epsilon$  has zero mean and correlation matrix  $R$ , as

$$(1) \quad E[yy^T] = E[A\epsilon\epsilon^T A^T] = AE[\epsilon\epsilon^T]A^T = AIA^T = R,$$

where  $I$  is the identity matrix. An ensemble of realizations generated this way will have exactly the required correlation structure. The method, however, is computationally very expensive even when the Toeplitz structure of  $R$  is exploited (a matrix is said to be Toeplitz if entries are equal along any diagonal parallel to the main diagonal). Indeed, if a Cholesky decomposition for  $R$  is used in (1) (such as in Ma, Wei, and Mills [13]), the best existing algorithm for calculating this factorization has a computational cost of  $O(m^2)$  flops (Kailath [16]), and calculation of each particular realization will require a further  $O(m^2)$  flops.

Given the high cost of matrix factorizations, modelers prefer faster methods, even if the correlation structure of the realizations produced by these methods only approximates the desired structure. Perhaps the most commonly used of these methods is the discrete spectral approximation of Shinozuka and Jan [25]. Very briefly, if  $r(|x|)$  has Fourier transform  $\tilde{r}(|\omega|)$  then the spectral representation theorem for stationary processes (Yaglom [33]) states that  $Y(x)$  can be written as

$$Y(x) = \text{Real} \left[ \int_{-\infty}^{\infty} \exp(2\pi i \omega x) dZ(\omega) \right],$$

where  $dZ(\omega)$  is a complex-valued Gaussian process with zero mean and variance  $E[|dZ(\omega)|^2] = \tilde{r}(|\omega|)d\omega$ . This representation suggests approximating  $Y(x)$  by the series

$$(2) \quad Y^*(x) = \text{Real} \left[ l^{-1/2} \sum_{k=-m}^m \epsilon_k \tilde{r}^{1/2}(|k/l|) \exp(2\pi i x k/l) \right],$$

where  $l$  is a length scale and the  $\epsilon_k$  are zero mean, independently and identically distributed (i.i.d.) complex-valued Gaussian random variables with unit variance.  $Y^*(x)$  can now be speedily calculated at equispaced points  $x_j = jl/m$  by use of the FFT in  $O(m \log m)$  flops. This is a substantial improvement on the cost of a matrix factorization.

Shinozuka and Jan [25] actually proposed the use of a slightly different approximation; we have presented (2) here in preference to their original approximation for two reasons. First, its output has a true Gaussian distribution, while the output of Shinozuka and Jan's method is only asymptotically Gaussian. Second, it better shows the relation between the spectral method and the new algorithm proposed here.

In either case though, while such spectral methods are fast, they are not exact. As  $Y^*(x)$  is only an approximation to the true process  $Y(x)$ , the vector  $y^* =$

$(Y^*(x_0), \dots, Y^*(x_m))^T$  will not have exactly the same correlation structure as  $y$ . As shown by Black and Freyberg [3], guaranteeing that the correlation structure of the realizations  $y^*$  is a sufficiently accurate approximation to  $R$  requires careful analysis and fine tuning of process parameters.

Therefore, in light of the above advantages and disadvantages, we propose a new method that combines the best features of both the spectral and the matrix factorization approaches: it factorizes a carefully chosen extension of  $R$  to produce random vectors with exactly the required correlation structure via FFT. More specifically, for one-dimensional (1-D) simulations we first embed the Toeplitz matrix  $R$  in a nonnegative definite, symmetric, and circulant  $2M \times 2M$  matrix  $S$ . The eigendecomposition of  $S$  can be computed in  $O(M \log M)$  flops and this is used to generate a square root of  $S$ . Multiplication of white noise by this square root can then be carried out via FFT in a further  $O(M \log M)$  flops, and results in a random vector  $z$  such that any sub-vector  $y$  of  $z$  of length  $m+1$  has correlation matrix  $R$ . Extension to multidimensional simulations over a parallelogram domain with regular mesh is straightforward.

This useful result does not seem to be widely known. Indeed, after discovering it, the only previous use of it or a close variation that the authors found in the literature is the method described by Woods [31] for generating realizations of two-dimensional (2-D) Markov random fields with correlation functions having finite support. More recently and independently of us, Wood and Chan [32] suggested circulant embeddings to generate stationary Gaussian processes.

Before closing this introduction, we have to mention that the turning bands method remains a valuable tool for stationary Gaussian fields sampled on a grid consisting of a large number of scattered nodes. This is also the case for the matrix factorization approach if the field is nonstationary and the number of sampling nodes small.

The paper is organized as follows. Section 2 defines the concept of a nonnegative definite circulant embedding and describes how to generate realizations of 1-D Gaussian processes once a nonnegative embedding has been found. Section 3 establishes conditions under which the minimal circulant embedding (in which  $M = m$ ) is nonnegative definite. This theory and supporting numerical calculations are used in section 4 to demonstrate that many of the commonly used correlation models for 1-D simulations have nonnegative definite minimal embeddings. Section 5 describes extension of the approach to higher-dimensional Gaussian processes and gives some numerical results on the existence of nonnegative embeddings for the associated correlation functions. In section 6, numerical illustrations are provided, starting with examples of 2-D realizations obtained by circulant embedding with various correlation functions. This follows with a comparisons between CPU run-times of our generation method and the matrix factorization approach in one dimension. Finally, section 7 contains further discussion and conclusions.

**2. Nonnegative definite embeddings in circulant matrices.** As noted in the previous section the correlation matrix  $R$  of the stationary process  $Y(x)$  with correlation function  $r(x)$  sampled on the equispaced mesh  $\Omega = \{x_0, \dots, x_m\}$  has entries  $R_{pq} = r(|x_p - x_q|)$ . It is therefore a nonnegative definite symmetric Toeplitz matrix and can be characterized by its first row  $r = (r_0, r_1, \dots, r_m)$ , where  $r_k = r(|x_0 - x_k|)$ . Now consider a  $2M \times 2M$  Toeplitz and symmetric matrix  $S$  whose first row  $s$  consists of the entries

$$(3) \quad \begin{aligned} s_k &= r_k, & k &= 0, \dots, m, \\ s_{2M-k} &= r_k, & k &= 1, \dots, m-1, \end{aligned}$$

where if  $M > m$  the entries  $s_{m+1}, \dots, s_{2M-m}$  are arbitrary, or conveniently chosen. Then  $S$  is circulant and any  $(m+1) \times (m+1)$  block along the main diagonal of  $S$  is just a copy of the matrix  $R$ . Being circulant,  $S$  has the eigendecomposition  $S = (1/2M)F\Lambda F^H$ , where  $F$  is the standard FFT matrix of size  $2M$  with entries  $F_{pq} = \exp(2\pi i pq/2M)$ ,  $F^H$  is the conjugate transpose of  $F$ , and  $\Lambda$  is a diagonal matrix whose diagonal entries form the vector  $\tilde{s} = Fs$  (Barnett [2]). Thus a necessary and sufficient condition for  $S$  to be nonnegative definite is that all the entries in  $\tilde{s}$  be nonnegative.

If an embedding of  $R$  in a nonnegative definite circulant matrix  $S$  has been found, a vector  $y \sim \mathcal{N}(0, R)$  can be generated as follows. Let  $\epsilon = \epsilon_1 + i\epsilon_2$  be a complex-valued random vector with  $\epsilon_1$  and  $\epsilon_2$  normal, zero mean and real random vectors of dimension  $2M$  such that  $E[\epsilon_j \epsilon_k^T] = \delta_{jk}I$  for  $j, k = 1, 2$ , where  $\delta_{jk}$  is the Kronecker delta. Then it is easy to show that the real and imaginary parts of the vector  $e = F(\Lambda/2M)^{1/2}\epsilon$  form two independent real random vectors that are both  $\mathcal{N}(0, S)$ . Thus the two vectors formed from the real and imaginary parts of any  $m+1$  consecutive entries of  $e$  are independent of each other and are each  $\mathcal{N}(0, R)$ . Hence they are two independent realizations of  $Y$  and display exactly the required correlation structure over the sampling points in  $\Omega$ . This demonstrates that for the cost of an initial complex-valued FFT of length  $2M$  to get  $\tilde{s}$ , pairs of independent real realizations of length  $m+1$  with the desired correlation structure can be computed at a cost of a complex-valued FFT of length  $2M$  per realization pair.

In summary, given a nonnegative definite circulant extension  $S$  of  $R$ , the algorithm generates the required random vector as follows:

- (a) Compute via the FFT the discrete Fourier transform  $\tilde{s} = Fs$  and form the vector  $(\tilde{s}/2M)^{1/2}$ .
- (b) Generate a vector  $\epsilon = \epsilon_1 + i\epsilon_2$  of dimension  $2M$  with  $\epsilon_1$  and  $\epsilon_2$  being two independent and real random variables each  $\sim \mathcal{N}(0, I)$ .
- (c) Compute the vector  $\tilde{e}$  with entries  $\tilde{e}_k = \epsilon_k(\tilde{s}/2M)^{1/2}$ .
- (d) Compute via the FFT the discrete Fourier transform  $e = F\tilde{e}$ . The real and imaginary parts of any consecutive  $m+1$  entries in  $e$  now yield two independent realizations of  $Y(x)$  over the sampling grid  $\Omega = \{x_0, \dots, x_m\}$ .
- (e) Go to (b).

**3. Nonnegative definite minimal embeddings.** The above algorithm is competitive only as long as a nonnegative definite embedding can be easily determined for which  $M$  is not too much larger than  $m$ . Dembo, Mallows, and Shepp [8] have shown that a positive definite embedding always exists for any strictly positive definite Toeplitz matrix  $R$ . Unfortunately their embedding is not easily constructed. More importantly, in their proof, the size  $M$  of the embedding is bounded above only by  $O(\kappa(R)m^2)$ , where  $\kappa(R)$  denotes the condition number equal to the ratio of the largest to smallest eigenvalues of  $R$ . The bound can be improved to  $O(\kappa(R)^{1/2}m^{5/4})$ , but this result is best possible for this particular proof technique and cannot be further improved to give a bound that is linear in  $m$  (Newsam and Dietrich [22]). Moreover, for correlation structures gotten by discretizing a process with a smooth correlation function,  $\kappa(R)$  itself is likely to grow as some polynomial in  $m$  (Reade [24]; Newsam [21]). Also, in the extreme case where  $R$  is only nonnegative and not strictly positive definite, Dembo, Mallows, and Shepp give an example for which no nonnegative definite circulant embedding exists.

Therefore, rather than seek a general embedding strategy applicable to any  $R$ , we instead look for conditions under which the minimal circulant embedding with

$M = m$  is nonnegative. In this case, from (3) the first row  $s$  of  $S$  is

$$(4) \quad s = (r_0, r_1, \dots, r_m, r_{m-1}, \dots, r_1).$$

In the remainder of this section, whenever reference is made to *the minimal embedding of a vector  $r$* , it will mean the embedding of  $R$  into  $S$  where  $R$  and  $S$  are, respectively, the symmetric Toeplitz matrices with first rows  $r$  and  $s$ , with  $s$  as defined in (4). We begin by noting the following theorem.

**THEOREM 1.** *Let  $r(x)$  be a nonnegative definite and symmetric function with Fourier transform  $\tilde{r}(\omega)$ . If the Fourier transform of  $\tilde{r}(\omega)$  recovers  $r(x)$  and  $\tilde{r}(\omega)$  is absolutely integrable and of bounded variation, the function*

$$(5) \quad \tilde{s}_l(\omega) = r(0) + 2 \sum_{k=1}^{\infty} r(k/l) \cos(2\pi k\omega)$$

*is uniformly convergent, uniformly continuous, and nonnegative for any length scale  $l$ .*

*Proof.* From Champeney ([5, p. 163, Theorem 15.16]) for any positive  $l$  the following holds true almost everywhere:

$$(6) \quad \begin{aligned} l \sum_{k=-\infty}^{\infty} \tilde{r}(x - kl) &= \sum_{k=-\infty}^{\infty} r(k/l) \exp(2\pi i k x l) \\ &= r(0) + 2 \sum_{k=1}^{\infty} r(k/l) \cos(2\pi k x l) \end{aligned}$$

with the second equality stemming from the symmetry of  $r(x)$ . Since Bochner's theorem ([5, p. 100]) implies that  $\tilde{r}(\omega)$  is nonnegative, (6) is nonnegative for any value  $x = \omega/l$ . Uniform convergence and continuity follow from the conditions on  $\tilde{r}(\omega)$ .  $\square$

The following corollary to Theorem 1 establishes the first situation in which the existence of nonnegative definite minimal embeddings is guaranteed.

**COROLLARY 1.** *If the function  $r(x)$  satisfies the conditions of Theorem 1 with  $r(x) = 0$  for  $|x| \geq l$ , then the vector  $r$  with entries  $r_k = r(k/l)$ ,  $k = 0, \dots, [l]$ , where  $[l]$  is the least integer greater than  $l$ , has a nonnegative definite minimal embedding.*

*Proof.* As  $r(x)$  satisfies the conditions of Theorem 1, the function  $\tilde{s}_l(\omega)$

$$\begin{aligned} \tilde{s}_l(\omega) &= r(0) + 2 \sum_{k=1}^{\infty} r(k/l) \cos(2\pi k\omega) \\ &= r_0 + 2 \sum_{k=1}^{[l]-1} r_k \cos(2\pi k\omega) + r_{[l]} \cos(2\pi [l]\omega) \end{aligned}$$

is nonnegative. This implies that the vector  $\tilde{s}$  having entries  $\tilde{s}_j = \tilde{s}_l(j/2[l])$  is nonnegative. But  $\tilde{s}$  is just the discrete Fourier transform of the vector  $s$  defined in (4), so the corollary is proven.  $\square$

The corollary shows that discrete realizations of any process whose correlation function has finite support can be generated via minimal embeddings as long as the realizations include enough points to cover the support of the function. The next corollary establishes a generalization of Corollary 1 by showing that, even if the correlation function does not have bounded support, minimal embeddings will still be nonnegative as long as  $\Omega$  is large enough relative the length scale  $l$ .

COROLLARY 2. Suppose that  $r(x)$  satisfies the conditions of Theorem 1 and that  $\tilde{s}_l(\omega)$  is strictly positive. Then for every  $l$  there exists a positive integer  $m$  that depends on  $l$  such that the vector  $r$  with entries  $r_k = r(k/l)$ ,  $k = 0, \dots, m$  has a nonnegative definite minimal embedding.

*Proof.* Since  $\tilde{s}_l(\omega)$  is uniformly continuous and strictly positive,  $\tilde{s}_l(\omega) \geq \epsilon$  for some  $\epsilon > 0$  and all  $\omega \in [0, 1]$ . Uniform convergence of (5) implies there exists an  $m$  such that  $|r(m/l)| \leq \epsilon/2$  and

$$\left| 2 \sum_{k=m+1}^{\infty} r(k/l) \cos(2\pi k\omega) \right| \leq \frac{\epsilon}{2}$$

for all  $\omega$ . If we define  $\tilde{s}_{l,m}(\omega)$  by

$$(7) \quad \tilde{s}_{l,m}(\omega) = r(0) + 2 \sum_{k=1}^{m-1} r(k/l) \cos(2\pi k\omega) + r(m/l) \cos(2\pi m\omega),$$

then the definition of  $m$  ensures that  $|\tilde{s}_l(\omega) - \tilde{s}_{l,m}(\omega)| \leq \epsilon$  for all  $\omega$ . Thus from the definition of  $\epsilon$ , it follows that  $\tilde{s}_{l,m}(\omega) \geq 0$ . Hence the vector  $\tilde{s}$  with entries  $\tilde{s}_j = \tilde{s}_{l,m}(j/2m)$  is nonnegative, which completes the proof.  $\square$

We thus see that if a correlation function satisfies the assumptions of Corollary 2, discrete realizations with this correlation function can be generated from minimal embeddings as long as they contain enough points. As an example, consider a realization with the commonly used exponential correlation function  $r(x) = e^{-x}$  to be generated on the points  $x_k = k/l$ . Let  $\nu = e^{-1/l}$ . Then from formula 1.353.3 in Gradshteyn and Ryzhik ([14, p. 31])

$$(8) \quad \tilde{s}_{l,m}(\omega) = \frac{(1 - \nu^2) \left( 1 - \nu^m \cos(2\pi m\omega) \right) + 2\nu^{m+1} \sin(2\pi\omega) \sin(2\pi m\omega)}{1 - 2\nu \cos(2\pi\omega) + \nu^2}.$$

The denominator in (8) is always positive, and the numerator will be positive if

$$1 - \nu^2 \geq \nu^m (1 + \nu)^2$$

or

$$(9) \quad 1 - \nu \geq 2\nu^m.$$

Thus choosing  $m$  so that  $m \geq l \log_e(2/(1 - \nu)) \approx l \log_e 2l$  for large  $l$  will ensure that the vector  $r$  with entries  $r_k = e^{-k/l}$ ,  $k = 0, \dots, m$  has a nonnegative definite minimal embedding. The Appendix establishes a similar result for the Gaussian correlation function  $r(x) = e^{-x^2}$ . More precisely, it shows that if  $l \geq \pi^{-1/2}$  and  $m \geq \pi^{1/2} l^2$  then the vector  $r$  with entries  $r_k = e^{-(k/l)^2}$ ,  $k = 0, \dots, m$  has a nonnegative definite minimal embedding. The numerical results in the next section indicate, however, that this bound is unduly pessimistic in practice.

A closer look at (8) shows that the bound derived from the definition of  $s$  in (3) is sufficient but not necessary. Since the first term in the numerator of (8) is always positive and the last term vanishes at  $\omega_j = j/2m$ , the elements of the vector  $\tilde{s}$  with entries  $\tilde{s}_j = \tilde{s}_{l,m}(j/2m)$  are nonnegative regardless of the values of  $m$  and  $l$ . Thus for this correlation function the minimal embedding is always nonnegative definite, even though  $\tilde{s}_{l,m}(\omega) < 0$  for some values of  $\omega$ ,  $m$  and  $l$ . A formula similar to (8)

can be calculated for the so-called *hole* correlation function  $r(x) = (1-x)e^{-x}$  which again shows that  $\tilde{s}_j \geq 0$  regardless of the values of  $m$  and  $l$ . Although the proof is straightforward, it is lengthy and for this reason is not given here.

The above results suggest that the existence of nonnegative definite minimal embeddings may be quite common. The next result, adapted from Zygmund ([35, Volume I, Chapter 5, Theorem 1.5]), shows that for a large class of correlation functions the minimal embedding is, indeed, always nonnegative definite.

**THEOREM 2.** *If the entries of the vector  $r = (r_0, \dots, r_m)$  form a sequence that is convex, decreasing, and nonnegative, then  $r$  has a nonnegative definite minimal embedding.*

*Proof.* It suffices to show that for any integer  $j$

$$(10) \quad \tilde{s}_j = r_0 - r_m(-1)^j + 2 \sum_{k=1}^m r_k \cos(2\pi jk/2m)$$

is nonnegative. We first define the finite differences  $\Delta r_k = r_k - r_{k+1}$ ,  $\Delta^2 r_k = \Delta r_k - \Delta r_{k+1}$ , and the Dirichlet and Féjer kernels

$$D_p(\omega) := \begin{cases} 1 + 2 \sum_{k=1}^p \cos(2\pi k\omega) = \frac{\sin \pi\omega(2p+1)}{\sin \pi\omega} & \text{if } p \geq 1, \\ 1 & \text{otherwise;} \end{cases}$$

$$K_p(\omega) := \sum_{k=0}^p D_k(\omega) = \left( \frac{\sin \pi\omega(p+1)}{\sin \pi\omega} \right)^2.$$

Upon summations by parts (10) can be rewritten as

$$(11) \quad \begin{aligned} \tilde{s}_j &= r_m(D_m(j/2m) - (-1)^j) + \sum_{k=0}^{m-1} \Delta r_k D_k(j/2m) \\ &= r_m(D_m(j/2m) - (-1)^j) + \Delta r_{m-1} K_{m-1}(j/2m) \\ &\quad + \sum_{k=0}^{m-2} \Delta^2 r_k K_k(j/2m). \end{aligned}$$

The last two terms in (11) are nonnegative since the entries in  $r$  define a convex and decreasing sequence and the Féjer kernels  $K_k$  are nonnegative. Also, the first term is nonnegative since  $r_m$  is nonnegative and  $D_m(j/2m) - (-1)^j$  is equal to  $2m$  if  $j = 0$  and zero otherwise. The theorem is therefore proved.  $\square$

We note in passing that the nonnegativity condition on  $r$  can be replaced by the weaker condition

$$r_0 + r_m + 2 \sum_{k=1}^{m-1} r_k \geq 0.$$

Finally the following simple result on the existence of minimal embeddings for products is also useful.

**THEOREM 3.** *If two vectors  $r_1$  and  $r_2$  of the same dimension have nonnegative definite minimal embeddings, the vector  $r$  formed by the product of the pairs of correspondent components of  $r_1$  and  $r_2$  also has a nonnegative definite minimal embedding.*

*Proof.* By the convolution theorem for finite sequences, the discrete Fourier transform  $\tilde{s}$  of the minimal embedding of  $r$  is the convolution of the discrete Fourier transforms  $\tilde{s}_1$  and  $\tilde{s}_2$  of the minimal embeddings of  $r_1$  and  $r_2$ . As all terms in both  $\tilde{s}_1$  and  $\tilde{s}_2$  are nonnegative, it follows that  $\tilde{s}$  must also be nonnegative.  $\square$

**4. Minimal embeddings of standard correlation models in one dimension.** We now consider minimal embeddings of sequences from correlation models of practical interest. The functions given below have all been proposed at one time or another as models for correlations in geostatistical simulations, in either one or more dimensions. In the latter case, radial symmetry is often assumed, with  $x$  being replaced by  $|x|$  indicating the distance between points:

exponential (see Tompson, Ababou, and Gelhar [27])

$$(12) \quad r(x) = e^{-x};$$

spherical (see Journel and Huijbregts [15])

$$(13) \quad r(x) = \begin{cases} 1 - \frac{3}{2}x + \frac{1}{2}(x)^3 & \text{if } 0 \leq x \leq 1, \\ 0 & \text{otherwise;} \end{cases}$$

power (see Mardia and Watkins [20])

$$(14) \quad r(x) = \begin{cases} (1-x)^\gamma & \gamma \geq 2 \quad \text{if } 0 \leq x \leq 1, \\ 0 & \text{otherwise;} \end{cases}$$

Gaussian (see Warnes [28])

$$(15) \quad r(x) = e^{-x^2};$$

Whittle (see Whittle [30])

$$(16) \quad r(x) = xK_1(x).$$

In the Whittle model (16),  $K_1(x)$  is the modified Bessel function of second kind and order 1. The Whittle model arises from solving in two dimensions the Laplace equation driven by white noise.

Since one application envisaged for the results presented in section 3 is in supplying 1-D realizations for the turning bands method, we also consider 1-D correlation functions  $r(x)$  derived from radially symmetric 2- and three-(3)-dimensional correlation models (denoted here by  $r_2(x)$  and  $r_3(x)$ , respectively) via the well-known relations (Christakos [6])

$$(17) \quad r(x) = \frac{d}{dx} \int_0^x \frac{ur_2(u)du}{(x^2 - u^2)^{1/2}},$$

$$(18) \quad r(x) = \frac{d}{dx}(xr_3(x)).$$

With this, the aim in this section was to check 1-D minimal embeddings for the above models. The correlation  $r(x)$  in (17) and (18) was computed with  $r_2(x)$  and  $r_3(x)$  being any of the models (12) to (16). For the Gaussian and Whittle models (15) and (16), the correlation  $r(x)$  in (17) was calculated numerically after making the change of variable  $u = x \sin \nu$ .

Each of the models (12), (13), and (14) satisfies the conditions of Theorem 2, which implies that each has nonnegative definite minimal embeddings. On the other hand, the Gaussian and Whittle models are not convex, so that Theorem 2 does not apply to them. In addition, even if  $r_2(x)$  or  $r_3(x)$  satisfies the conditions of Theorem



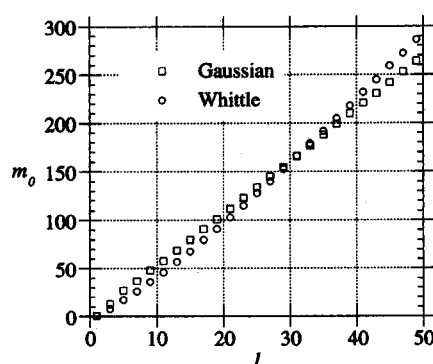


FIG. 1. Given  $l$ , smallest value  $m_0$  of  $m$  for which the minimal embedding is nonnegative for the 1-D Gaussian and Whittle models (15) and (16), respectively.

2, it does not follow that the corresponding function  $r(x)$  generated by (17) or (18) will also satisfy these conditions. For example, if  $r_3(x) = \exp(-x)$  then  $r(x)$  is the so-called hole effect  $(1-x)\exp(-x)$ , and this function is neither convex, positive, nor everywhere decreasing. However, as indicated in section 3, any vector  $r$  constructed from the hole effect has a nonnegative minimal embedding. For these reasons, when results could not be derived directly from the theory given in section 3, numerical experiments were conducted. This applied to the Whittle model (16) and for the correlations  $r(x)$  obtained from (17) and (18) with  $r_2(x)$  and  $r_3(x)$  being one of the five correlation models (12) to (16). Also, the Gaussian model (15) was included to check the validity of the bound derived in the Appendix.

For these cases, we calculated in double precision (real\*12) the discrete Fourier transform  $\tilde{s}$  for minimal embeddings of a range of vectors  $r$ . For successive integer length scales  $l$  between 1 and 50, vectors  $r$  with entries  $r_k = r(k/l)$ ,  $k = 0, \dots, m$  were defined for  $m$  taking on successive integer values between 1 and 400. When the power model was used in (17) and (18), calculations were done for the exponents  $\gamma = 2, 3, 4, 5$ , and 6. From these experiments, the only correlations for which any vectors  $\tilde{s}$  registered negative values were those involving the Gaussian and Whittle models. This is illustrated in Figure 1 where for each value of  $l$  the smallest value  $m_0$  of  $m$  for which the minimal embedding is nonnegative is shown. It is interesting to note that for the values of  $l$  invoked, the relationship between  $l$  and  $m_0$  is close to linear, implying that the bound derived for the Gaussian model in the Appendix may be overly pessimistic in practice.

Note that these numerical results suggest that some extension of Theorem 2 may hold generally for functions derived by (17) or (18) from models that themselves satisfy Theorem 2, but we have not been able to prove this.

**5. Extension to multidimensional simulations.** Consider first 2-D simulations. Under the assumption of stationarity, the random field  $Y(x, y)$  has correlation function  $r(x, y)$ . Let  $\Delta x$  and  $\Delta y$  be constants denoting, respectively, the horizontal and vertical mesh size of a 2-D rectangular sampling grid  $\Omega$  formed by the points  $(x_p, y_q)$ , where  $x_p = p\Delta x$  and  $y_q = q\Delta y$  with  $0 \leq p \leq m$  and  $0 \leq q \leq n$ . In this paper, the ordering of the grid nodes is done from left to right, bottom to top.

With this, the correlation matrix  $R$  is block Toeplitz with each block being Toeplitz (Zimmerman [34]). Therefore, being also symmetric,  $R$  is uniquely char-

acterized by its first block row

$$(19) \quad (R_0, R_1, \dots, R_n),$$

with each block  $R_j$  for  $j = 0, \dots, n$  being square of dimension  $m + 1$ . Note that with our node ordering, the blocks  $R_j$  have first row and first column entries, respectively, given by

$$(20) \quad \{r(i\Delta x, j\Delta y)\}_{i=0}^m \quad \text{and} \quad \{r(-i\Delta x, j\Delta y)\}_{i=0}^m.$$

The idea now is to embed each  $R_j$  in a square circulant matrix  $S_j$ . To do so, the procedure of section 2 has to be extended as, in view of (20), for  $j \geq 1$  the blocks  $R_j$  are symmetric only if the correlation function has the special form  $r(|x|, |y|)$ . This is done as follows for each  $R_j$ . Being Toeplitz,  $R_j$  is uniquely characterized by its first row and first column which are written, respectively, as

$$(21) \quad (r_{0j}, r_{1j}, \dots, r_{mj}) \quad \text{and} \quad (r_{0j}, r_{-1j}, \dots, r_{-mj})^T.$$

The minimal circulant embedding of  $R_j$  that ensures that the embedding matrix has an even dimension (for FFT computation) is then given by the square circulant matrix  $S_j$  of dimension  $2(m + 1)$ , for which the first row is

$$(22) \quad (r_{0j}, r_{1j}, \dots, r_{mj}, \phi_j, r_{-mj}, \dots, r_{-1j}),$$

where  $\phi_j$  is in principal arbitrary but here is chosen equal to  $(r_{mj} + r_{-mj})/2$ . Thus, for any correlation function  $r(x, y)$  each block  $R_j$  in (19) can be embedded in a square circulant matrix  $S_j$  of dimension  $2(m + 1)$ . Let  $\bar{S}$  be the block Toeplitz matrix with first block row and first block column being, respectively,

$$(23) \quad (S_0, S_1, \dots, S_n) \quad \text{and} \quad (S_0, S_1^T, \dots, S_n^T)^T.$$

Clearly,  $\bar{S}$  is an embedding of  $R$  with the property that its blocks are circulant. There remains, however, to extend  $\bar{S}$  to a matrix  $S$  that is also block circulant. This is done for (23) by following exactly the procedure that led from (21) to (22). In other words, the matrix  $S$  is taken as the block circulant matrix with first block row

$$(24) \quad (S_0, S_1, \dots, S_n, \Phi, S_n^T, \dots, S_1^T)$$

with  $\Phi = (S_n + S_n^T)/2$ . Here, the inclusion of  $\Phi$  ensures that  $m$  and  $n$  can always be chosen so that the dimension of  $S$  is a power of 2 (or at least a product of small prime numbers) for fast FFT computations. With this,  $S$  is an embedding of  $R$ , has dimension  $d = 4(m + 1)(n + 1)$  and is block circulant with all its blocks being circulant.

As we did for the 1-D case, let  $r$  and  $s$  denote the first row of  $R$  and  $S$ , respectively. Given that the major computational effort in our methodology is the calculation of  $s$ , i.e., that of the first row of (24), observe that  $s$  is indeed very easily computed: (20) to (22) yield the first row of  $S_j$  while, being the first columns of  $S_j$ , the first row of  $S_j^T$  is simply the first row of  $S_j$  in reverse order, except for the first row entry which remains unchanged.

With this, if  $F$  is the 2-D discrete Fourier transform matrix,  $S$  has the eigenvalue decomposition  $S = (1/d)F\Lambda F^H$  with  $\Lambda$  being diagonal and the eigenvalues on its diagonal forming the vector  $\tilde{s} = Fs$ . Thus if all components in  $\tilde{s}$  are nonnegative, the decomposition  $S = (1/d)F\Lambda^{1/2}(F\Lambda^{1/2})^H$  is possible, and the argument given in section 2 carries through. In other words, if  $\epsilon = \epsilon_1 + i\epsilon_2$  is a random complex

vector of dimension  $d$  with  $\epsilon_1$  and  $\epsilon_2$  being real normal random variables with zero mean and  $E[\epsilon_i \epsilon_j^T] = \delta_{ij} I$ , the real and imaginary parts of the vector  $e = F\tilde{e}$  with  $\tilde{e} = (\Lambda/d)^{1/2} \epsilon$  yield two real and independent random vectors that are both  $\mathcal{N}(0, S)$ . As  $R$  is embedded in  $S$ , extraction from  $e$  of two random vectors that are distributed as  $\mathcal{N}(0, R)$  is straightforward.

Computational requirements are as follows. The products  $Fs$  and  $F\tilde{e}$  can be computed by the FFT. This means that the computation of realizations of  $Y$  over the grid  $\Omega$ , will be dominated by one FFT of dimension  $d$  to first get  $\tilde{s} = Fs$  and, thereafter, one single FFT of dimension  $d$  for each pair of independent realizations. This represents an overall cost of  $O(d \log_2 d)$  floating point operations per realization. The storage requirements are a single complex array of dimension  $d$ .

As in one dimension, our approach is only valid if all components in  $\tilde{s}$  are nonnegative. Fortunately a number of the results in section 3 have straightforward extensions to higher dimensions. For correlation functions with bounded support contained in the interval  $[0, l_1] \times [0, l_2]$ , where  $l_1$  and  $l_2$  denote the length scales in the horizontal and vertical dimensions, generalization of Corollary 1 to two dimensions shows that the minimal embedding will be nonnegative definite if  $l_1 \leq |x_0 - x_m|$  and  $l_2 \leq |y_0 - y_n|$ . This applies in particular to the spherical and power models of the previous section. Likewise, since the Fourier transform is separable, any separable correlation function whose 1-D components have nonnegative definite embeddings will also have a nonnegative embedding. In particular the results of section 3 on the exponential function  $r(x) = e^{-|x|/l}$  show that the 2-D separable, anisotropic correlation function  $r(x, y) = e^{-|x|/l_1 - |y|/l_2}$  will always admit a nonnegative definite minimal embedding.

For correlation functions with infinite support, the 2-D equivalent of Corollary 2 indicates that provided the size of the sampling grid is sufficiently large compared correlation length scales, the vector  $r$  will have a nonnegative definite and minimal embedding. As in the previous section, some guide on the required sampling size can be gained from numerical experiments in which the discrete Fourier transform  $\tilde{s}$  of minimal embeddings is calculated for a range of vectors  $r$ . This was done for the exponential (12), Gaussian (15), and Whittle (16) correlation functions over a square grid  $\Omega$ , i.e.,  $m = n$ . In particular, for successive integer length scales  $l$  between 1 and 20, the vector  $r$  with entries  $r_{pq} = r((p^2 + q^2)^{1/2}/l)$ ,  $p, q = 0, \dots, m$  was defined for  $m$  taking on successive integer values until the associated minimal embedding was nonnegative. For each of the three correlation functions and each value of  $l$ , the smallest  $m$  (denoted  $m_0$ ) for which the minimal embedding of  $r$  was nonnegative definite is plotted in Figure 2. As was the case in section 4, for these values of  $l$  the relationship between  $l$  and  $m_0$  appears to be close to linear.

For the Gaussian model, as  $m$  increases the smallest elements in  $\tilde{s}$  decayed very quickly to the level of machine precision and so displayed a random pattern of positive and negative signs. For this reason, the effect of round-off errors needed to be filtered out. This was done by increasing the first component of the vector  $r$  by a very small amount equal to  $10^{-12}$ . In the geostatistical literature, such a perturbation in the correlation function is usually called a *nugget* effect (Journel and Huijbregts [15]). Again, all computations were performed in double precision (Real\*12).

Extension of the approach to 3-D problems is straightforward once it is realized that over a 3-D rectangular and regularly meshed sample grid  $\Omega$ , the correlation matrix of the process will be block symmetric and block Toeplitz with each block having all the properties of the correlation matrix in two dimensions. Thus, the embedding strategy of  $R$  into  $S$  carries through with realizations of the process being generated

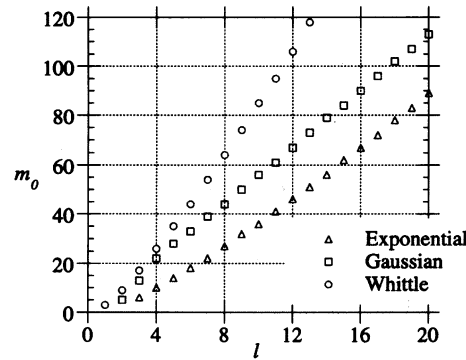


FIG. 2. Given  $l$ , smallest value  $m_0$  of  $m$  for which the minimal embedding is nonnegative for the 2-D exponential, Gaussian, and Whittle models (12), (15), and (16), respectively.

by 3-D FFTs. Also, the approach extends to a computationally efficient generation of conditional simulations (see Dietrich and Newsam [11]).

If simulations are required over a grid that is regularly meshed but with an irregular boundary, it is always possible to embed the irregularly shaped grid into a rectangular mesh  $\Omega$  and to apply the approach on  $\Omega$ . Furthermore, although the sampling grid has been so far assumed to have a rectangular mesh, the circulant embedding approach remains valid for a parallelogram mesh, as in such a case  $R$  retains its Toeplitz/block Toeplitz structure (Zimmerman [34]).

Finally, note that if the correlation function is of the form  $r(|x|, |y|)$ , then (22) can be replaced by (4) and (24) can be replaced by

$$(S_0, S_1, \dots, S_n, S_{n-1}, \dots, S_1)$$

leading to a matrix  $S$  of smaller dimension  $d = 4mn$  (see Dietrich and Newsam [10] for further details).

## 6. Illustrations.

**6.1. Computation of 2-D realizations.** We provide here two applications of our circulant embedding approach to the generation of stationary random fields. We first start with realizations of a 2-D random log hydraulic conductivity field often required in the modeling of groundwater systems [17, 23]. Letting  $Y(x, y)$  denote the log hydraulic conductivity at a point  $(x, y)$  of the groundwater domain, it is usually assumed that  $Y(x, y)$  is Gaussian with mean  $\mu(x, y)$ . Furthermore, field stationarity is generally invoked on some portion of the groundwater domain. With this, the computation of log hydraulic conductivity values often amounts to generate over a regularly meshed grid  $\Omega$ , realizations of a zero-mean field  $Y(x, y) - \mu(x, y)$  with correlation function  $r(x, y)$ .

To illustrate our approach, we have generated over a rectangular 2-D grid  $\Omega$  with unit mesh and size  $m = 511, n = 383$ , zero mean log hydraulic realizations with the two following correlation functions,

$$(25) \quad r(x, y) = e^{-(\mathbf{z} \mathbf{A} \mathbf{z}^T)^{1/2}},$$

$$(26) \quad r(x, y) = e^{-\frac{|x|}{l_1} - \frac{|y|}{l_2}},$$

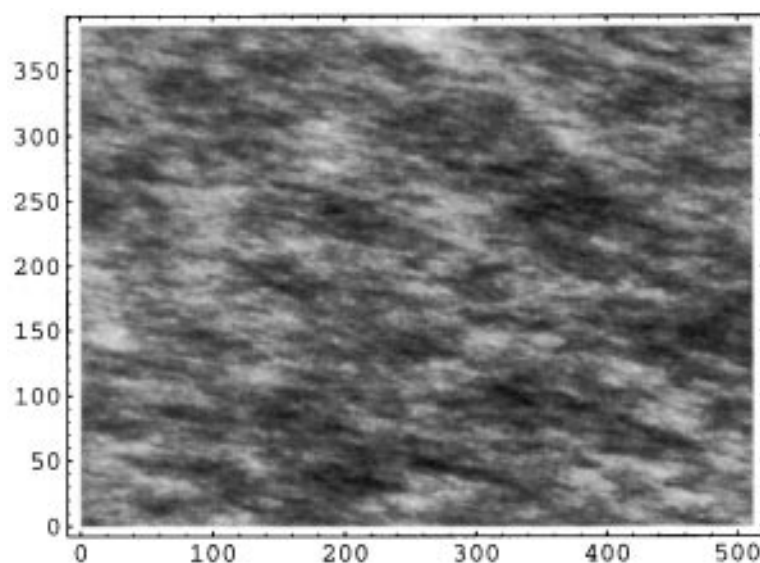


FIG. 3. Realization of a field with the anisotropic exponential correlation (25) over a 2-D grid with unit mesh and size  $m = 511, n = 383$ .

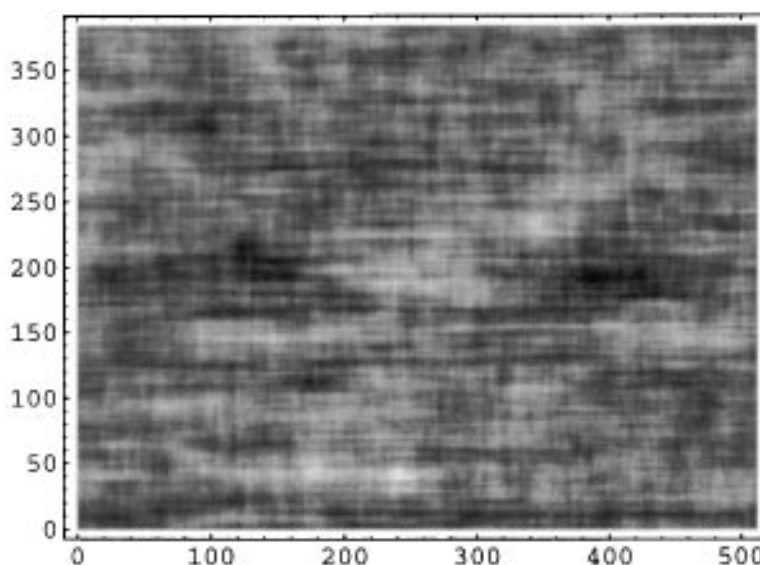


FIG. 4. Realization of a field with the separable, anisotropic exponential correlation (26) over a 2-D grid with unit mesh and size  $m = 511, n = 383$ .

where in (25)  $\mathbf{z} = (x/l_1, y/l_2)$  and  $A$  is the symmetric, positive definite matrix

$$A = \begin{pmatrix} 3 & 1 \\ 1 & 2 \end{pmatrix}.$$

The length scales were set to  $l_1 = 50$  and  $l_2 = 15$ . Realizations are shown as density plots in Figures 3 and 4.

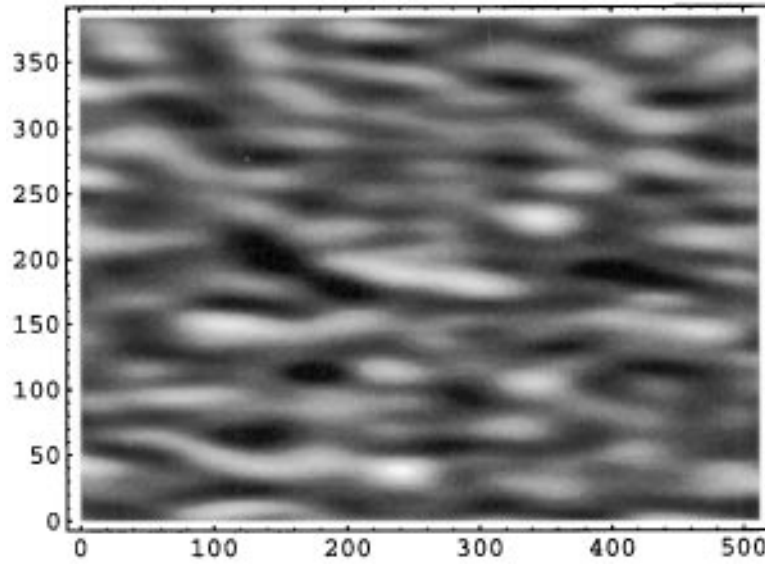


FIG. 5. Realization of a field with the Gaussian-based correlation (27) over a 2-D grid with unit mesh and size  $m = 511, n = 383$ .

Observe that for (25) we have  $r(-x, y) \neq r(x, y)$ , implying that the blocks  $R_j$  for  $j \geq 1$  in (19) are not symmetric. In this case, however, from an eigenvalue decomposition of  $A$  it is easy to find a coordinate transformation (symmetry and/or rotation) such that in the transformed system, the correlation depends only on the absolute value of its two arguments. For this reason, we have considered an instance for which such a coordinate transformation is not possible in the form of the correlation model

$$(27) \quad r(x, y) = \left(1 - \frac{x^2}{l_1^2} - \frac{xy}{l_1 l_2} - \frac{y^2}{l_2^2}\right) e^{-\frac{x^2}{l_1^2} - \frac{y^2}{l_2^2}}$$

based on the function

$$-\frac{1}{4} \left( \frac{\partial^2}{\partial x^2} + \frac{\partial^2}{\partial x \partial y} + \frac{\partial^2}{\partial y^2} \right) e^{-x^2 - y^2} = (1 - x^2 - xy - y^2) e^{-x^2 - y^2}$$

which, from inspection of the spectral density, can be seen to be an appropriate correlation function. A realization plot for (27) with the same setting as that of Figures 3 and 4 is shown in Figure 5.

It is worth noting that, as shown in Dietrich [12, section 3.2, p. 151], the popular turning band method very often invoked by geostatisticians cannot generate reasonably accurate field realizations with the separable correlation function (26) since the required line correlation solution to (17) is infinite at the origin. On the other hand, as indicated in the previous section, (26) always admits a nonnegative definite minimal embedding.

The Fortran source code required to generate the above 2-D realizations is very simple and amounts to only a few dozen lines. Implementation was on a Macintosh LC 630 (full 68040 chip, 20 Mb RAM) with the IMSL routine `fft2d` invoked for 2-D FFT computation. CPU time for each realization was only a few minutes including

I/O. The embeddings for (27) had some negative eigenvalues, but these were near machine precision and so could be set to zero without affecting in a significant way the accuracy of the simulation.

As a second example, we have considered the generation of fully developed non-Gaussian random sea wave slopes often required in sea glitter modeling. As shown in Wegener, Dietrich, and Newsam [29], random sea wave slopes  $\nabla H(x, y)$ , where  $H$  denotes sea wave height, can be constructed from a nonlinear transformation of a Gaussian and stationary vector-valued field  $\mathbf{Y}(x, y) = (Y_1(x, y), Y_2(x, y))$ . As a consequence, a component of the approach described in [29] was to extend the circulant embedding algorithm of section 5 valid for a scalar field  $Y(x, y)$  to a circulant embedding algorithm for  $\mathbf{Y}(x, y)$ . This extension was straightforward and the reader will find in Figure 6 a density plot of a realization of a sea wave slope  $\nabla H(x, y)$ . In this figure, the sea surface is driven by a wind speed of 10 meter/sec blowing from left to right. The sea domain is a 2-D rectangular grid with mesh and domain size equal, respectively, to  $5 \times 5$  and  $1275 \times 955$  square meters, i.e.,  $m = 255, n = 191$ .

**6.2. CPU timing.** We provide here CPU run-time for the generation of a zero-mean, stationary, and 1-D process  $Y(x)$  sampled on a set of equispaced points  $\Omega = \{x_0, \dots, x_m\}$  on the line. In this exercise, the circulant approach is compared to the Cholesky factorization approach. For the latter, the Cholesky factor was computed in  $O(m^2)$  flops using a displacement representation of the Toeplitz correlation matrix  $R$  (Lev-Ari and Kailath [18]). Realizations sizes were set to  $m = 2^k$  with  $k$  taking successive integer values between 8 and 15.

Results obtained with the above-mentioned Macintosh LC 630 are plotted in Figure 7 with  $k = \log_2 m$  on the horizontal axis and  $\log_2$  of the CPU run-time expressed in seconds on the vertical axis. As expected, this figure shows that with  $m$  increasing, the CPU run-times for the circulant and Cholesky approaches are indeed proportional to  $m \log m$  and  $m^2$ , respectively.

**7. Discussion.** We have presented a method that will, under suitable assumptions, produce realizations of a stationary and possibly anisotropic random process at minimal cost. Moreover we have demonstrated that it can be applied to generate realizations with many of the standard correlation functions used in geostatistical simulations. In particular, the results in section 3 prove that in one dimension, minimal embeddings are guaranteed to be nonnegative definite for many correlation functions, regardless of the length of the sequence embedded. Furthermore, Corollary 2 indicates that, even if not all sequences from a particular function have nonnegative definite embeddings, if the sequence samples cover a distance significantly greater than the length scale of the correlation function then the minimal embedding is very likely to be nonnegative definite. For such functions the algorithm is clearly superior to other commonly used methods: it has the same computational cost as the spectral method while being more accurate, and it is as accurate as the matrix factorization method while being considerably easier to implement and having a much lower computational cost.

The question of characterizing further classes for which results similar to those of Theorem 2 can be proven remains open, but some observations can be made. In particular, in one dimension, convexity in a neighborhood of the origin appears to be necessary to guarantee a nonnegative definite embedding for every  $m$  and  $l$ . To see this, consider an everywhere twice differentiable correlation function  $r(x)$ . Symmetry implies that  $r'(x)$  must vanish at the origin. Furthermore let  $\tilde{r}(\omega)$  be the Fourier transform of  $r(x)$ . Since  $r(x)$  is positive definite, Bochner's theorem implies that  $\tilde{r}(\omega)$

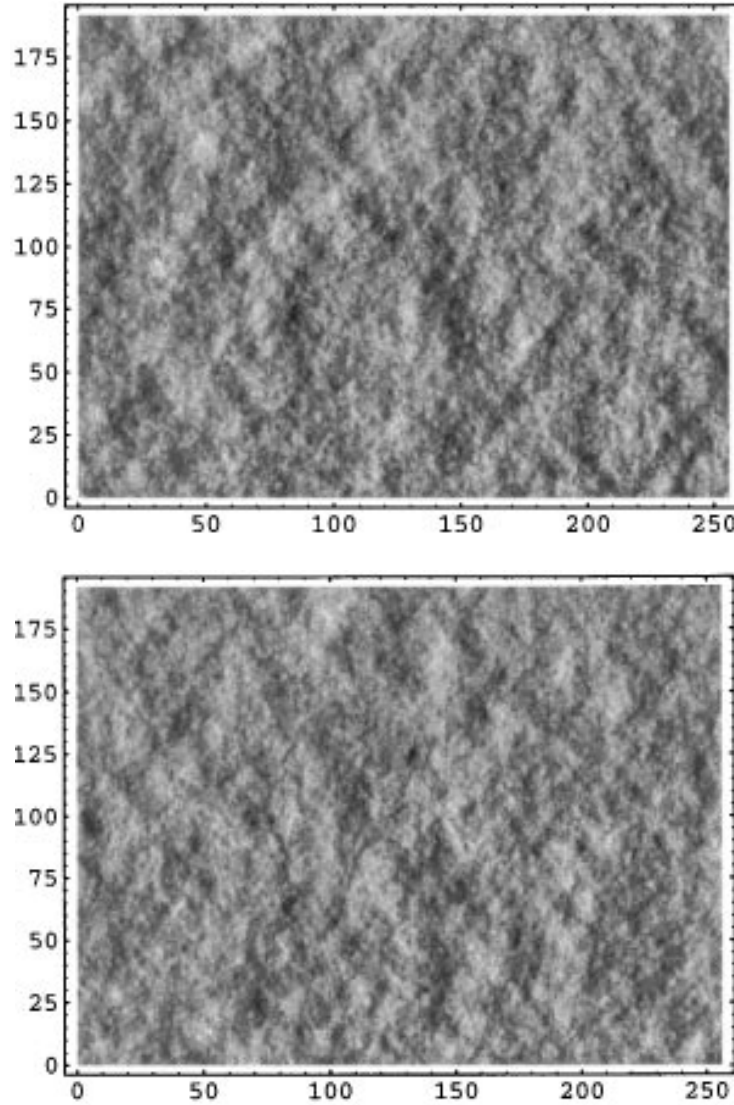


FIG. 6. Realization of random sea wave slope  $\nabla H(x, y) = (H_x, H_y)$  used in the modeling of sea glitter over a 2-D sea surface grid with mesh and domain size equal, respectively, to  $5 \times 5$  and  $1275 \times 955$  square meters, i.e.,  $m = 255, n = 191$ .  $H_x$  and  $H_y$  are, respectively, the first and second plot in this figure.

is nonnegative. Since  $r''(0) = -4\pi^2 \int_R \omega^2 \tilde{r}(\omega) d\omega$ ,  $r''(0)$  must be strictly less than zero. Thus  $r(x)$  is concave in a neighborhood of the origin and looks locally like the function  $r^+(x) = 1 - \eta x^2$  with  $\eta > 0$ . A little calculation shows that the trigonometric polynomial associated with a minimal embedding of a sequence from this function is

$$\begin{aligned}
 \tilde{s}_{l,m}(\omega) &= 1 + (1 - \eta(m/l)^2) \cos(2\pi m\omega) + 2 \sum_{k=1}^{m-1} (1 - \eta(k/l)^2) \cos(2\pi k\omega) \\
 &= \sin(2\pi m\omega) \cot(\pi\omega) + \eta \left( \sin(2\pi m\omega) \cot(\pi\omega) \csc^2(\pi\omega) \right. \\
 &\quad \left. + 4m \cos(2\pi m\omega) \csc^2(\pi\omega) - 4m^2 \sin(2\pi m\omega) \cot(\pi\omega) \right) / (2l)^2.
 \end{aligned}
 \tag{28}$$



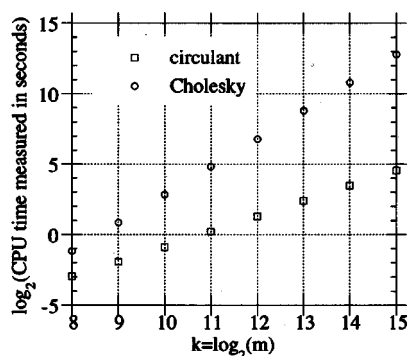


FIG. 7. Comparison of CPU run-times to generate a 1-D realization with exponential correlation via the  $O(m \log_2 m)$  circulant approach and a  $O(m^2)$  Cholesky approach.

Now only the third term in (28) does not vanish at the points  $\omega_j = j/2m, j \neq 0$ . As it alternates in sign,  $r^+$  cannot have a nonnegative definite embedding for any choice of  $\eta$ ,  $m$ , and  $l$ . Thus, given any smooth correlation function for sufficiently small values of  $m$  and large values of  $l$ , the minimal embedding will look like (28) and alternate in sign. In contrast, convexity in a neighborhood of the origin forces  $r(x)$  to have a discontinuous derivative at the origin in the form of a corner or a cusp.

Finally, we would like to find further conditions that ensure the existence of embeddings in higher dimensions. Unfortunately results here are mixed. On the one hand Theorems 1 and 3 and the two corollaries have natural extensions to two or more dimensions. On the other hand, for each of the standard 2-D correlation functions considered in section 4, numerical experiments found certain values of  $m$  and  $l$  for which the minimal embeddings failed to be nonnegative definite. As noted in section 5, in practice minimal embeddings are still nonnegative for many values of  $m$  and  $l$  of interest; it seems, however, that a more subtle theory will be needed to justify this. One possible and interesting approach to this is to use a more sophisticated form of embedding than (4), such as the one used by Dembo, Mallows, and Shepp [8].

**Appendix.** This Appendix derives bounds on the size  $m$  of circulant embeddings of the Gaussian correlation function  $r(x) = \exp(-x^2)$  needed to guarantee nonnegativity. The definitions and notation for elliptic functions used in the derivations here are those given in Abramowitz and Stegun [1], with additional results as needed from Gradshteyn and Ryzhik [14]. First, a given length scale  $l$  defines a nome  $\nu \leq 1$  through  $\nu = \exp(-1/l^2)$ . Thus for the Gaussian correlation function, definitions (5) and (7) become

$$(A1) \quad \begin{aligned} \tilde{s}_l(\omega) &= 1 + 2 \sum_{k=1}^{\infty} \nu^{k^2} \cos(2\pi k\omega), \\ \tilde{s}_{l,m}(\omega) &= 1 + 2 \sum_{k=1}^{m-1} \nu^{k^2} \cos(2\pi k\omega) + \nu^{m^2} \cos(2\pi m\omega). \end{aligned}$$

Equation (A1) is just the definition of the theta function  $\theta_3(\pi\omega)$  [1, (16.27.3)], and the alternative expansion [14, (8.181.2)]

$$\theta_3(\pi\omega) = \prod_{k=1}^{\infty} (1 + 2\nu^{2k-1} \cos 2\pi\omega + \nu^{2(2k-1)})(1 - \nu^{2k})$$

shows that the minimum of  $\tilde{s}_l(\omega)$  occurs at  $\omega = 1/2$  and has value  $\theta_3(\pi\omega) = \theta_4(0) = (2(1-\eta)^{1/2}K(\eta)/\pi)^{1/2}$  [14 (8.183.4); 1, (16.38.8)]. Here  $K(\eta)$  is the complete elliptic integral with parameter  $\eta$  [1, (16.1.1)], and  $\eta$  is determined by  $l$  by inversion of the following equation, derived from the relation between the nome and the complete elliptic integral [1, (17.3.17)]:

$$(A2) \quad l^2 = \frac{K(\eta)}{\pi K(1-\eta)}.$$

Next, a sufficient condition for an embedding of length  $m$  to be nonnegative definite is that  $\tilde{s}_{l,m}(\omega) \geq 0$ , and this will be ensured if  $|\tilde{s}_l(\omega) - \tilde{s}_{l,m}(\omega)| \leq \min_{\omega} \tilde{s}_l(\omega)$  for all  $\omega$ . But

$$\begin{aligned} |\tilde{s}_l(\omega) - \tilde{s}_{l,m}(\omega)| &= \left| \nu^{m^2} \cos(2\pi m\omega) + 2 \sum_{k=m+1}^{\infty} \nu^{k^2} \cos(2\pi k\omega) \right| \\ &\leq \nu^{m^2} \left( 1 + 2 \sum_{k=1}^{\infty} \nu^{k^2} \right) \\ &= \nu^{m^2} \theta_3(0) = \nu^{m^2} (2K(\eta)/\pi)^{1/2}. \end{aligned}$$

Thus a sufficient condition for a nonnegative definite minimal embedding is to choose  $m$  so that  $\nu^{m^2} \theta_3(0) \leq \theta_4(0)$ , or, equivalently,  $\nu^{m^2} (2K(\eta)/\pi)^{1/2} \leq (2(1-\eta)^{1/2}K(\eta)/\pi)^{1/2}$ . Cancelling the common term and taking logs of both sides of this inequality yields

$$(A3) \quad \frac{m^2}{l^2} \geq -\frac{\log(1-\eta)}{4}.$$

We now seek an upper bound for  $\log(1-\eta)$  in terms of  $l$  to substitute into (A3). First, suppose that  $l \geq \pi^{-1/2}$ . Then Figure 17.1 and (17.3.33) in [1] show that this assumption implies that  $K(1-\eta) \leq 2$ . Moreover, (17.3.33) also gives the bound  $K(\eta) \geq 1 - 0.5 \log(1-\eta)$ . Substituting these bounds into (A2) gives

$$\frac{1 - 0.5 \log(1-\eta)}{2\pi} \leq l^2,$$

which implies

$$-\log(1-\eta) \leq 4\pi l^2 - 2.$$

Therefore, substituting back into (A3), it suffices to choose  $m$  so that

$$\frac{m^2}{l^2} \geq \frac{4\pi l^2 - 2}{4} \geq -\frac{\log(1-\eta)}{4},$$

which finally gives the following sufficient condition on  $m$  and  $l$  to ensure a nonnegative definite minimal embedding:  $m \geq \pi^{1/2} l^2$  for  $l \geq \pi^{-1/2}$ . This bound can be asymptotically improved to  $m \geq \pi l^2/2$  for  $l$  sufficiently large as  $K(1-\eta) \sim \pi/2$  as  $\eta \rightarrow 1$ . Nevertheless, Figure 1 suggests that this bound is unduly pessimistic, and a bound that is essentially linear in  $l$  may hold in practice.

#### REFERENCES

- [1] M. ABRAMOWITZ AND I. A. STEGUN, *Handbook of Mathematical Functions*, Dover, New York, 1970.
- [2] S. BARNETT, *Matrices, Methods and Applications*, in Oxford Applied Mathematics and Computing Sciences Series, Clarendon Press, Oxford, 1990.

- [3] T.C. BLACK AND D.L. FREYBERG, *Simulation of one-dimensional correlated fields using a matrix-factorization moving average approach*, Math. Geol., 22 (1990), pp. 39–62.
- [4] L. BORGMAN, M. TAHERI, AND R. HAGAN, *Three-dimensional frequency-domain simulations of geological variables*, in Geostatistics for Natural Resource Characterization, Part 2, G. Verly, M. David, A. G. Journel, and A. Marechal, eds., Reidel, Dordrecht, the Netherlands, 1984, pp. 517–541.
- [5] D.C. CHAMPENEY, *A Handbook of Fourier Theorems*, Cambridge University Press, London, 1987.
- [6] G. CHRISTAKOS, *The space transformation in the simulation of multi-dimensional random fields*, Math. Comput. Simulation, 29 (1987), pp. 313–319.
- [7] M.W. DAVIS, *Production of conditional simulations via the LU triangular decomposition of the covariance matrix*, Math. Geol., 19 (1987), pp. 91–98.
- [8] A. DEMBO, C.L. MALLOWS, AND L.A. SHEPP, *Embedding nonnegative definite Toeplitz matrices in nonnegative definite circulant matrices, with application to covariance estimation*, IEEE Trans. Inform. Theory, IT-35 (1989), pp. 1206–1212.
- [9] C.R. DIETRICH, *Computationally efficient Cholesky factorization of a covariance matrix with block Toeplitz structure*, J. Statist. Comput. Simulation, 45 (1993), pp. 203–218.
- [10] C.R. DIETRICH AND G.N. NEWSAM, *A fast and exact method for multidimensional Gaussian stochastic simulations*, Water Resour. Res., 29 (1993), pp. 2861–2869.
- [11] C. R. DIETRICH AND G. N. NEWSAM, *Fast and exact method for multidimensional Gaussian stochastic simulations: extension to conditional simulations*, Water Resour. Res., 32 (1996), pp. 1643–1652.
- [12] C. R. DIETRICH, *A simple and efficient space domain implementation of the turning bands method*, Water Resour. Res., 31 (1995), pp. 147–156.
- [13] F. MA, M. S. WEI, AND W.H. MILLS, *Correlation structuring and the statistical analysis of steady-state groundwater flow*, SIAM J. Sci. Statist. Comput., 8 (1987), pp. 848–867.
- [14] I. S. GRADSHTEYN AND I. M. RYZHIK, *Table of Integrals, Series, and Products*, Academic Press, New York, 1979.
- [15] A.G. JOURNEL AND C.T. HUIJBREGTS, *Mining Geostatistics*, Academic Press, New York, 1978.
- [16] T. KAILATH, *A theorem of I. Schur and its impact on modern signal processing*, in Schur Methods in Operator Theory and Signal Processing, I, I. Gohberg, ed., Birkhauser-Verlag, Basel, 1986, pp. 9–30.
- [17] P.R. KING AND P.J. SMITH, *Generation of correlated properties in heterogeneous porous media*, Math. Geol., 20 (1988), pp. 863–877.
- [18] H. LEV-ARI AND T. KAILATH, *Triangular factorization of structured matrices*, in I. Schur Methods in Operator Theory and Signal Processing, I. Gohberg, ed., Birkhauser-Verlag, Basel, 1986, pp. 301–324.
- [19] A. MANTOGLU AND J.L. WILSON, *The turning bands method for simulation of random fields using line generation by a spectral method*, Water Resour. Res., 18 (1982), pp. 1379–1394.
- [20] K.V. MARDIA AND A.J. WATKINS, *On the multimodality of the likelihood in the spatial linear model*, Biometrika, 76 (1989), pp. 289–295.
- [21] G.N. NEWSAM, *On the asymptotic distribution of the eigenvalues of discretizations of a compact operator*, in Proc. Center for Mathematical Analysis, Vol. 17: Special Program on Inverse Problems, Australian National University, Canberra, Australia, 1988.
- [22] G.N. NEWSAM AND C.R. DIETRICH, *Bounds on the size of nonnegative definite circulant embeddings of positive definite Toeplitz matrices*, IEEE Trans. Inform. Theory, 40 (1994), pp. 1218–1220.
- [23] B.S. RAMARAO, A. M. LAVENUE, G. DE MARSILY, AND M. G. MARIETTA, *Pilot point methodology for automated calibration of an ensemble of conditionally simulated transmissivity fields*, 1. *Theory and computational experiments*, Water Resour. Res., 31 (1995), pp. 475–493.
- [24] J.B. READE, *On the sharpness of Weyl's estimates for eigenvalues of smooth kernels*, SIAM J. Math. Anal., 19 (1988), pp. 627–631.
- [25] M. SHINOZUKA AND C.M. JAN, *Digital simulation of random processes and its applications*, J. Sound Vibrations, 25 (1972), pp. 111–128.
- [26] G. SPOSITO, W. A. JURY, AND V.K. GUPTA, *Fundamental problems in the stochastic convection-dispersion model of solute transport in aquifers and field soils*, Water Resour. Res., 22 (1986), pp. 77–88.
- [27] A.F.B. TOMPSON, R. ABABOU, AND L.W. GELHAR, *Implementation of the three-dimensional turning bands field generator*, Water Resour. Res., 25 (1989), pp. 2227–2243.
- [28] J.J. WARNES, *A sensitivity analysis for universal kriging*, Math. Geol., 18 (1986), pp. 653–676.

- [29] M. WEGENER, C. R. DIETRICH, AND G. N. NEWSAM, *Generation of non-Gaussian sea surfaces for IR scene simulations*, Infrared Technology XXI, SPIE's 1995 International Symposium on Optical Science, Engineering and Instrumentation, San Diego, CA, 1995.
- [30] P. WHITTLE, *On stationary processes in the plane*, Biometrika, 41 (1954), pp. 434–449.
- [31] J.W. WOODS, *Two-dimensional discrete Markovian fields*, IEEE Trans. Inform. Theory, 18 (1972), pp. 101–109.
- [32] A. WOOD AND A. CHAN, *Simulation of Stationary Gaussian Processes in  $[0, 1]^d$* , Report CMA-SR06-93, Centre for Mathematics and Its Applications, Australian National University, Canberra, Australia, 1993.
- [33] A.M. YAGLOM, *Correlation Theory of Stationary and Related Random Functions*, Springer-Verlag, New York, 1987.
- [34] D.L. ZIMMERMAN, *Computationally exploitable structure of covariance matrices and generalized covariance matrices in spatial models*, J. Statist. Comput. Simulation, 32 (1989), pp. 1–15.
- [35] A. ZYGMUND, *Trigonometric Series*, Cambridge University Press, London, 1959.